

# **$\beta$ Klotho inhibits androgen/androgen receptor-associated epithelial-mesenchymal transition in prostate cancer through inactivation of ERK1/2 signaling**

ZHAO LIU<sup>1,2</sup>, HUI ZHANG<sup>3</sup>, SENTAI DING<sup>2</sup>, SHASHA QI<sup>3</sup>, SHUAI LIU<sup>2</sup>, DINGQI SUN<sup>2</sup>,  
WEI DONG<sup>2</sup>, LEI YIN<sup>2</sup>, MINGJIANG LI<sup>3</sup>, XINGBO ZHAO<sup>3</sup> and JIAJU LU<sup>2</sup>

<sup>1</sup>Department of Urology, Qilu Hospital of Shandong University, Jinan, Shandong 250012; Departments of <sup>2</sup>Urology, and <sup>3</sup>Obstetrics and Gynecology, Shandong Provincial Hospital Affiliated to Shandong University, Jinan, Shandong 250021, P.R. China

Received November 18, 2017; Accepted April 4, 2018

DOI: 10.3892/or.2018.6399

**Abstract.** The epithelial-mesenchymal transition (EMT) is reported to have intimate crosstalk with androgen receptor (AR) signaling in prostate cancer (PCa) and is known to be responsible for castration resistance. Fibroblast growth factor/receptor (FGF/FGFR) signaling is also involved in tumor progression and EMT in multiple tissues. Several studies have investigated the role of  $\beta$ Klotho, an FGF/FGFR signaling co-receptor in tumorigenesis. However, its role in PCa remains unknown. In the present study, the role of androgen in the EMT of PCa cells was examined by western blotting. The expression of  $\beta$ Klotho was examined in prostate cells and PCa tissues by western blotting and immunohistochemistry, respectively. The biological role of  $\beta$ Klotho was revealed by a series of functional *in vitro* and *in vivo* studies. We determined that  $\beta$ Klotho expression was significantly decreased in PCa tissues compared with benign prostatic hyperplasia (BPH) tissues, and low  $\beta$ Klotho expression was associated with a high Gleason score of PCa.  $\beta$ Klotho overexpression inhibited the viability, migration, and androgen/AR-associated EMT of PCa cells through the inactivation of ERK1/2 signaling. Notably,  $\beta$ Klotho overexpression inhibited prostate tumor growth and EMT *in vivo*. Knockdown of  $\beta$ Klotho produced the opposite effects. In conclusion,  $\beta$ Klotho inhibits EMT and plays a tumor-suppressive role in PCa, linking FGF/FGFR/ $\beta$ Klotho signaling to the regulation of PCa progression.

## **Introduction**

Prostate cancer (PCa) is the most commonly diagnosed cancer and the second leading cause of cancer-related mortality among the male population in Western countries (1). Androgen-deprivation therapy (ADT) is a standard of care treatment for recurrent or advanced PCa, and it efficiently controls the growth of androgen-dependent tumors. However, most of these tumors may eventually relapse in a castration-resistant fashion during ADT, which is defined as castration-resistant prostate cancer (CRPC) (2). Multiple studies have revealed that epithelial-mesenchymal transition (EMT) plays an important role in the development of drug-resistance and CRPC (3). EMT was initially identified as a developmental process during which epithelial cells acquire a migratory and invasive mesenchymal phenotype (4). The gene expression profile during EMT includes the decreased expression of epithelial genes, such as E-cadherin, and the increased expression of mesenchymal genes, such as N-cadherin and vimentin (5,6). Several transcription factors, such as Snail, Slug, Twist and Zeb1, have been linked to the induction of EMT under different cellular contexts (7-10).

A series of studies have revealed an intimate crosstalk between androgen receptor (AR) signaling and EMT, but the conclusions are controversial. Zhu and Kyprianou (11) demonstrated that AR expression was inversely correlated with androgen-induced EMT, indicating that low AR content facilitates the EMT phenotype. Additionally, a more recent study revealed that AR signaling was inversely correlated with Snail expression and disruption of AR-induced Snail-mediated EMT (12). In contrast to the aforementioned studies, others have reported that AR signaling has a stimulatory role in EMT (13,14). Collectively, these studies have reported inconsistent findings regarding the connection between AR signaling and the EMT phenotype, which warrants further clarification.

There is compelling evidence for aberrant fibroblast growth factor (FGF) signaling in the pathogenesis and progression of many cancers that originate from different tissue types. Feng *et al* (15) demonstrated that FGF19 was expressed in

---

*Correspondence to:* Dr Jiaju Lu, Department of Urology, Shandong Provincial Hospital Affiliated to Shandong University, 324 Jingwu Road, Jinan, Shandong 250021, P.R. China  
E-mail: kyoto2310@sina.com

**Key words:** prostate cancer,  $\beta$ Klotho, AR, FGF, EMT

primary and metastatic PCa tissues, and exogenous FGF19 promoted PCa progression. Studies in transgenic mice have revealed that the induction of FGFR1 activation can lead to irreversible prostate adenocarcinoma EMT and promote PCa development (16). Additionally, FGFR4 has been reported to promote EMT in PCa (17). Although numerous studies have linked FGFR-signaling activation to tumor progression, FGFR signaling has tumor-suppressive functions in certain contexts. Huang *et al* reported that FGFR4 limits hepatocarcinogenesis (18). In addition, it was reported that FGFR2-IIIb was downregulated during the progression of bladder cancer (19) and PCa (20). Collectively, the role of FGF/FGFR signaling in tumor is complex and varies in different contexts.

As one of the FGF/FGFR signaling co-receptors,  $\beta$ Klotho (KLB) can form a  $\beta$ Klotho/FGF19/FGFRs complex to exert its physiological function of energy metabolism and bile acid homeostasis (21-23). Notably,  $\beta$ Klotho has been investigated in several cancer studies. Ye *et al* (24) demonstrated that  $\beta$ Klotho suppresses tumor growth in hepatocellular carcinoma. In accordance with this finding, we (25) previously reported that  $\beta$ Klotho facilitated the inhibitory role of metformin in endometrial adenocarcinoma. However, another study revealed that  $\beta$ Klotho had an oncogenic role in hepatocellular carcinoma (26). Therefore, the exact role of  $\beta$ Klotho in tumorigenesis is debatable, and we are curious as to whether  $\beta$ Klotho plays a role in PCa.

In the present study, we found that androgen treatment induced EMT in the context of AR absence and a high AR content suppressed the androgen-induced EMT phenotype in PCa cells. Notably, we found that  $\beta$ Klotho acted as a suppressor of androgen/AR-associated EMT in PCa, and  $\beta$ Klotho may be a potential target for CRPC treatment.

## Materials and methods

**Reagents and antibodies.** DHT, U0126 and anti-AR antibodies (1:1,000 for western blot analysis; cat. no. A9853) were purchased from Sigma-Aldrich (Merck KGaA, Darmstadt, Germany). The anti-E-cadherin (1:1,000 for western blot analysis; 1:200 for IHC; cat. no. ab1416), N-cadherin (1:1,000 for western blot analysis, 1:200 for IHC; cat. no. ab98952), vimentin (1:1,000 for western blot analysis; cat. no. ab8978) and  $\beta$ Klotho antibodies (1:1,000 for western blot analysis; 1:100 for IHC; cat. no. ab106794) were purchased from Abcam (Cambridge, MA, USA). The anti-ERK1/2 (1:1,000 for western blot analysis; cat. no. 4695), phospho-ERK1/2 (Thr202/Tyr204) (1:1,000 for western blot analysis; cat. no. 4376), Slug (1:1,000 for western blot analysis; cat. no. 9585) and Snail (1:1,000 for western blot analysis; 1:200 for IHC; cat. no. 3879) antibodies were purchased from Cell Signaling Technology, Inc. (Danvers, MA, USA). The anti- $\beta$ -actin (1:1,000 for western blot analysis; cat. no. TA-09) and GAPDH antibodies (1:1,000 for western blot analysis; cat. no. TA08) and HRP-conjugated goat anti-rabbit and HRP-conjugated goat anti-mouse antibodies were purchased from ZSGB-BIO (Beijing, China).

**Tissue collection and immunohistochemistry analysis.** Human benign prostatic hyperplasia (BPH) samples were obtained from the transition zone of the prostate through

the transurethral resection of the prostate (TURP) surgery. Human prostate cancer (PCa) samples that were obtained from the tumor site during the surgery of radical prostatectomy (RP), were determined using the preoperative digital rectal examination (DRE) and magnetic resonance imaging (MRI). The final diagnosis was confirmed by two pathologists who were blind to the clinical or pathological data. None of the participants received any hormonal therapy prior to their operations. The study was approved by the Institutional Research Ethics Committees of Shandong Provincial Hospital Affiliated to Shandong University, and written informed consent was obtained from all patients. The protocol and analysis of immunohistochemistry was performed as previously described (25).

**Cell cultures and treatments.** The human PCa cell lines (PC3, LNCaP and C4-2B) and immortalized prostate epithelial cell line RWPE1 were purchased from the American Type Culture Collection (ATCC, Manassas, VA, USA). All cell lines were verified by short-tandem repeat (STR) profiling using Beijing Microread Gene Technology Co., Ltd. (Beijing, China). PCa cells were maintained in RPMI-1640 medium, supplemented with 10% fetal bovine serum (FBS) and 1% penicillin/streptomycin at 37°C in a humidified environment with 95% air and 5% CO<sub>2</sub>. RWPE1 cells were cultured in keratinocyte serum-free medium supplemented with bovine pituitary extract and epidermal growth factor from Invitrogen (Carlsbad, CA, USA). In the assays with the dihydrotestosterone (DHT) treatment, cells were pre-treated with 3% CSS (phenol free RPMI-1640 medium, supplemented with 3% charcoal-stripped FBS and 1% penicillin/streptomycin). DHT was dissolved in ethanol at a stock concentration of 10 mM and stored at -80°C. U0126, a specific MAPK/ERK inhibitor, was dissolved in dimethyl sulfoxide (DMSO) at a stock concentration of 20 mmol/l and stored at 4°C. Mock treatments with an identical volume of ethanol or DMSO were used as controls.

**Generation of the stably transfected cell clone.** The PC3 cells were plated on 6-well plates in 2 ml of culture medium containing 10% FBS and were transfected with 2  $\mu$ g of the GV230-CON083 plasmid [empty vector (EV)] or 2  $\mu$ g of the GV230- $\beta$ Klotho plasmid/well using the X-tremeGENE HP DNA Transfection reagent (Roche, Rotkreuz, Switzerland) according to the manufacturer's protocol. The plasmids were constructed by GeneChem Co., Ltd. (Shanghai, China). Twenty-four hours after transfection, the cells were placed under 500 mg/l geneticin (G418-sulfate; Gibco; Invitrogen) selection for 14 days. Individual colonies were removed by trypsinization and expanded. The G418-resistant PC3 clones were maintained in medium containing geneticin at 250 mg/l.

**siRNA transfection.** Cells were transfected with siRNAs using siLentFect Lipid reagent (Bio-Rad, Laboratories, Inc., Hercules, CA, USA) according to the manufacturer's protocol. The cells were incubated with the transfection complex, and the gene knockdown efficiency was assessed after 48 h. siRNAs were synthesized by GenePharma (Shanghai, China). The  $\beta$ Klotho siRNA sequence was, 5'GGAGAUGGAAGAGCUAUAUTT3' and the control siRNA sequence was, 5'UUCUCCGAACGUGUCACGUTT3'.

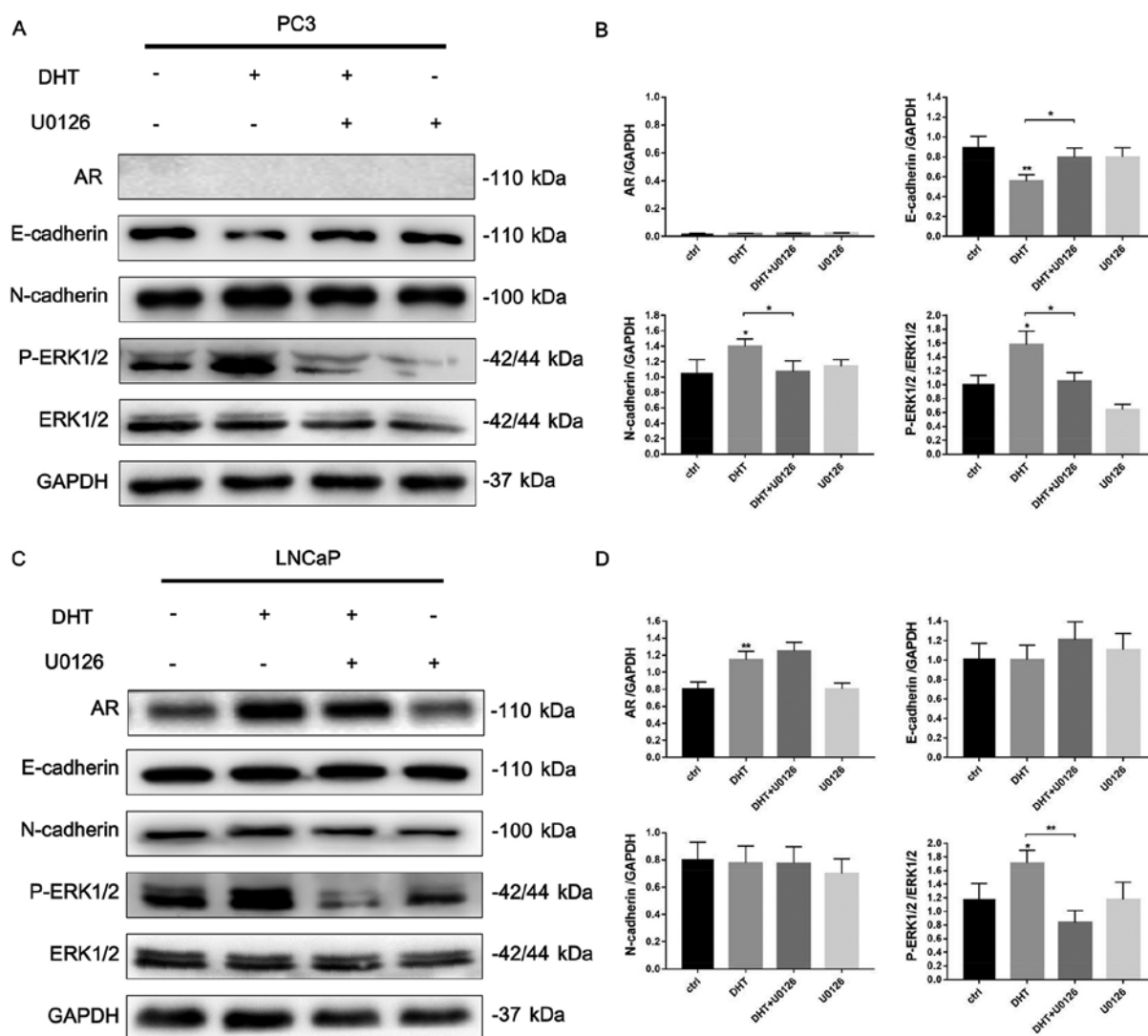


Figure 1. DHT induces EMT in AR-negative prostate cancer cells involving the ERK1/2 signaling pathway. (A) AR-negative PC3 cells were pretreated with 3% CSS for 24 h. Then the cells were treated with DHT (10 nM), U0126 (10  $\mu$ M) or both agents for 48 h. The protein expression of AR, E-cadherin, N-cadherin, p-ERK1/2, ERK1/2 and GAPDH were evaluated by western blotting. GAPDH was used as the loading control. (B) Quantification of the protein expression of PC3 cells was analyzed. (C) AR-positive LNCaP cells were treated in the same way as PC3 cells. (D) Quantification of the protein expression of LNCaP cells was analyzed. DHT, dihydrotestosterone; EMT, epithelial-mesenchymal transition; AR, androgen receptor; CSS, charcoal-stripped fetal bovine serum; U0126, ERK1/2 inhibitor. \*P<0.05, \*\*P<0.01 vs. untreated cells.

**Transwell assays.** The Transwell migration and invasion assays were performed using 24-well plates with 8- $\mu$ m pore size inserts (Corning Life Sciences, Corning, NY, USA) according to the manufacturer's instructions. The quantification was performed as previously described (25).

**Colony formation assay.** The PC3 cells ( $2 \times 10^3$ /well) were plated on a 60-mm dish in triplicate in 3 ml of medium containing 10% FBS and allowed to grow for 7 days. The culture medium was replaced every 3 days. The quantification was performed as previously described (25).

**Cell viability assay.** Cell viability was assessed using Cell Counting Kit (CCK)-8 (Tongren, Shanghai, China). Briefly, the cells were plated on 96-well plates in 100  $\mu$ l of medium (PC3,  $1 \times 10^3$  cells/well; and LNCaP,  $2 \times 10^3$  cells/well). Then, 10  $\mu$ l of CCK-8 reagent was added to each well at the indicated time-points (0, 24, 48 and 72 h), and the plates were incubated

at 37°C for 1 h. The optical density (OD) at 450 nm was measured in each well using a microplate reader. The experiments were repeated 3 times, and each assay was performed in triplicate.

**Apoptosis assay.** The PE Annexin V Apoptosis Detection kit I (BD Biosciences, Franklin Lakes, NJ, USA) was used to assess apoptosis according to the manufacturer's instructions. Briefly, the cells ( $1 \times 10^7$ ) were collected, washed with cold phosphate-buffered saline (PBS), gently resuspended in Annexin V binding buffer, and incubated with PE Annexin V/7-AAD. Flow cytometry was performed using the CellQuest Pro software (BD Biosciences). The experiments were repeated 3 times.

**Protein extraction and western blot analysis.** The cells ( $1 \times 10^7$ ) were harvested by centrifugation (1,000 rpm for 5 min) and washed with PBS. The cells were lysed in RIPA

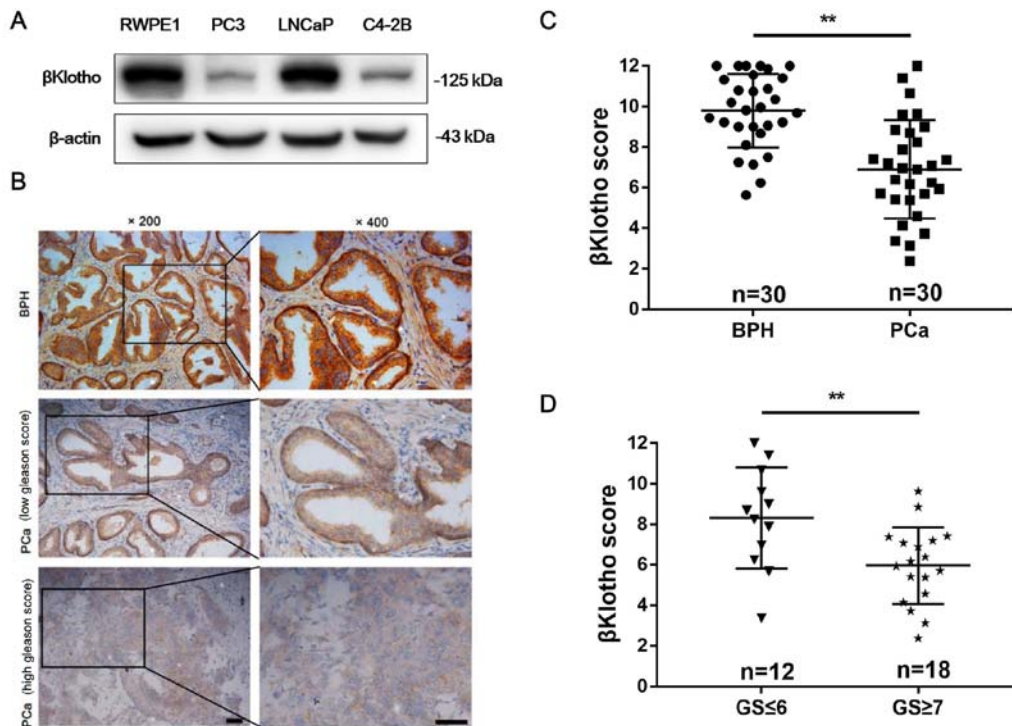


Figure 2.  $\beta$ Klotho expression in prostate cells and prostate tissues. (A) The protein expression of  $\beta$ Klotho in prostate epithelial RWPE1 cells and prostate cancer cells (PC3, LNCaP and C4-2B) was presented by western blotting.  $\beta$ -actin was used as the loading control. (B) Representative immunohistochemical staining of  $\beta$ Klotho in BPH (upper), low-grade PCa (middle) and high-grade PCa (lower) tissues. (C) The immunohistochemical score of  $\beta$ Klotho was calculated in BPH (n=30) and PCa (n=30) tissues. (D) The immunohistochemical score of  $\beta$ Klotho was calculated in low-grade PCa (GS  $\leq 6$ , n=12) and high-grade PCa (GS  $\geq 7$ , n=18) tissues. Data is presented as the mean  $\pm$  SD. Scale bar, 50  $\mu$ m; BPH, benign prostatic hyperplasia; PCa, prostate cancer; GS, Gleason score. \*\*P<0.01.

buffer containing protease inhibitors. Equal amounts of the protein lysates were electrophoretically separated on 10% SDS-PAGE gels and transferred to polyvinylidene fluoride (PVDF) membranes. The membranes were blocked with 5% non-fat milk in Tris-buffered saline/0.1% Tween-20 for 1 h at room temperature and then incubated overnight at 4°C with the primary antibodies. After incubation with the secondary antibody for 1 h at room temperature, the protein bands were detected using the ECL detection system (BD Biosciences).  $\beta$ -actin or GAPDH was used as the loading control. The experiment was performed 3 times.

**In vivo tumor model.** To obtain PC3 xenograft tumors,  $1 \times 10^6$  PC3-EV or PC3- $\beta$ Klotho cells with 100  $\mu$ l Matrigel (BD Biosciences) were subcutaneously inoculated in the flanks of 6- to 8-week-old BALB/c nude mice. Each experimental group consisted of eight mice. The tumor size in the mice and the mice body weight were assessed weekly. Tumor volume was calculated using the formula  $V = a \times b^2/2$ , where V is the volume ( $\text{mm}^3$ ), and a and b are the long and short diameter of the tumor (mm), respectively. After 4 weeks, the xenografts were harvested and analyzed by immunohistochemistry. Animals were maintained and handled according to the Animal Experiment guidelines of Shandong Provincial Hospital. The protocol was approved by our Institutional Committee.

**Statistical analysis.** The statistical analyses were performed using SPSS 19.0 (SPSS, Inc., Chicago, IL, USA). The values are expressed as the means  $\pm$  SD. The differences between

the two groups were determined by two-tailed Student's t-test. A P-value <0.05 was considered to indicate a statistically significant difference.

## Results

**DHT induces EMT in PC3 cells involving the regulation of the ERK1/2 signaling pathway.** To determine whether DHT is involved in the EMT regulation of PCa, we examined the expression of EMT-related markers in AR-negative PC3 (Fig. 1A and B) and AR-positive LNCaP (Fig. 1C and D) cell lines after DHT treatment using western blot analysis. DHT treatment significantly decreased the expression of E-cadherin and increased the expression of N-cadherin in PC3 cells. Next, we explored the possible signaling pathways that may be involved in this phenotype. We found that DHT significantly induced the phosphorylation of ERK1/2. In addition, after adding 10  $\mu$ M of U0126, an ERK1/2 signaling inhibitor, the DHT-induced downregulation of E-cadherin and upregulation of N-cadherin were reversed. Although DHT treatment induced AR expression and phosphorylation of ERK1/2 in AR-positive LNCaP cells, no significant effect was noted on the expression of EMT-related markers. Collectively, these data revealed that DHT treatment induced EMT through ERK1/2 signaling in the context of AR absence, and high AR content may reverse the DHT-induced EMT phenotype.

**$\beta$ Klotho expression in prostate cells and tissues.** As shown in Fig. 2A,  $\beta$ Klotho expression was determined in prostate epithelial RWPE1 cells and different PCa cell lines using



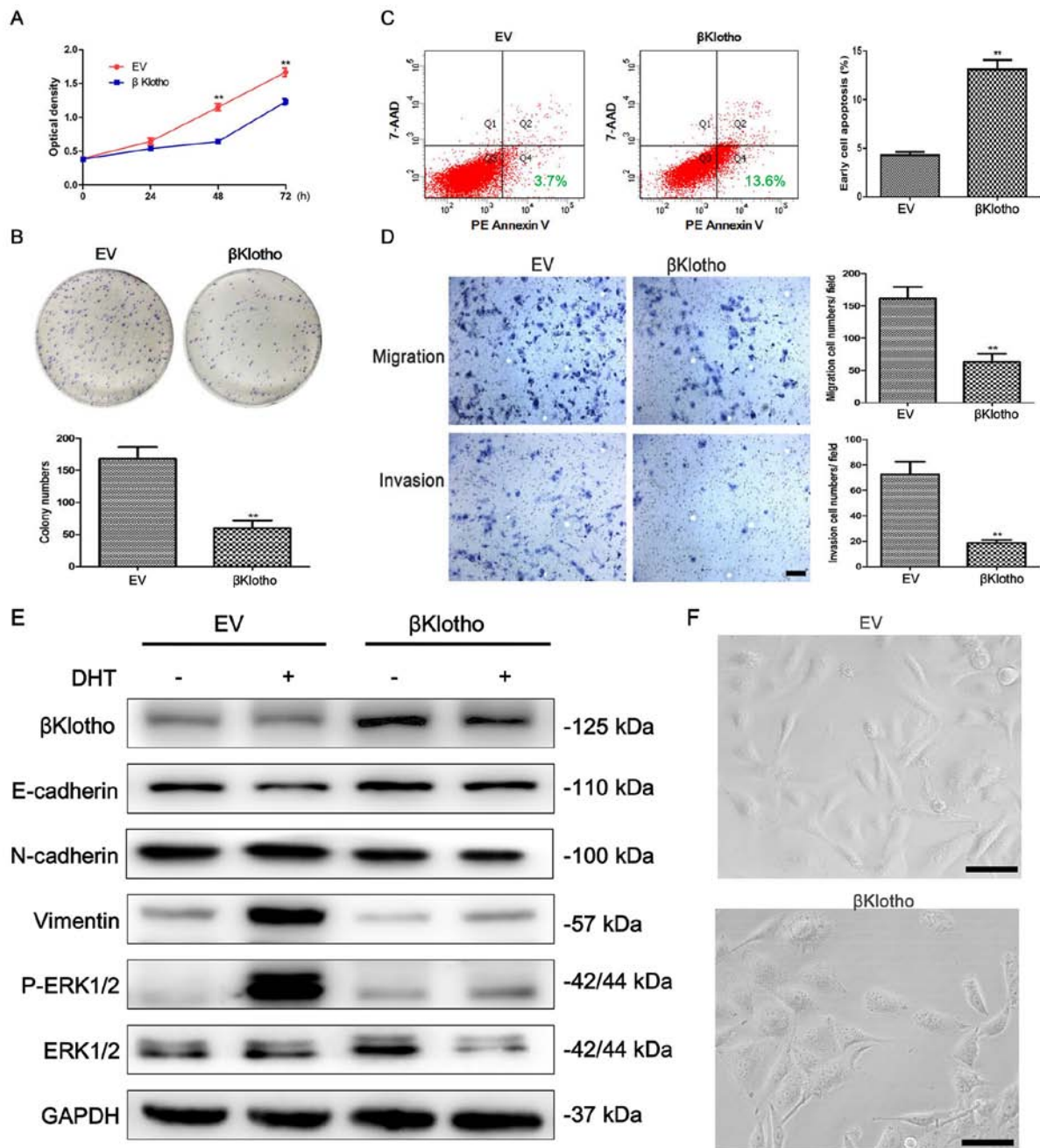


Figure 3. The effects of βKlotho overexpression in PC3 cells. PC3 cells were transfected with either EV or βKlotho. (A) A CCK-8 assay, (B) a colony formation assay, (C) an apoptosis assay and (D) Transwell migration and invasion assays were performed at the indicated times. (E) PC3-EV and PC3-βKlotho cells were treated with 3% CSS for 24 h, then the cells were treated with or without 10 nM of DHT for 48 h. Western blotting was performed to detect the expression of βKlotho, E-cadherin, N-cadherin, vimentin, p-ERK1/2 and ERK1/2. GAPDH was used as the loading control. (F) The morphology of PC3 cells transfected with either EV or βKlotho. The cells were observed using phase contrast microscopy at x200 magnification. Scale bar, 50 μm; \*\*P<0.01 vs. EV. DHT, dihydrotestosterone; CSS, charcoal-stripped fetal bovine serum.

western blot analysis. All of these 4 cell lines expressed βKlotho. Compared with RWPE1 and LNCaP cells, PC3 and C4-2B cells exhibited lower βKlotho expression. Next, we investigated the βKlotho expression in 30 human BPH and 30 PCa tissues by immunohistochemistry analysis. As shown in Fig. 2B, βKlotho was located in the cytoplasm and cytomembrane of both epithelial and stromal cells. BPH exhibited stronger βKlotho immunostaining compared with PCa tissues (Fig. 2C). In addition, the βKlotho expression in low-grade PCa (Gleason score ≤6) was stronger than that in high-grade PCa (Gleason score ≥7) (Fig. 2D). These data

indicated that βKlotho was downregulated in PCa tissues and that low βKlotho expression was associated with high Gleason score of PCa.

*βKlotho overexpression inhibits viability, migration and invasion and promotes apoptosis of PC3 cells.* Stable clones were generated to determine the effect of βKlotho expression on the viability, migration, invasion and apoptosis of PCa PC3 cells. Using a CCK-8 assay, we determined that βKlotho expression significantly reduced the viability of PC3 cells (Fig. 3A). This inhibitory effect of βKlotho expression on cell viability was

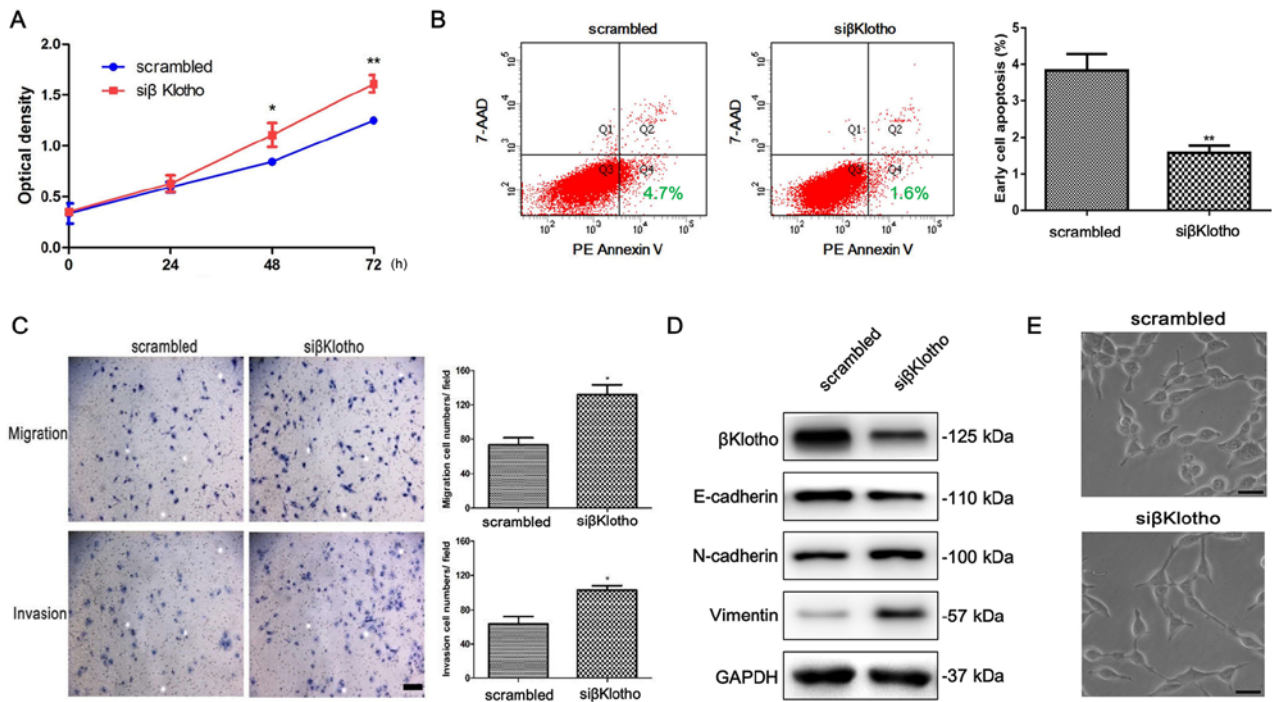


Figure 4. The effects of  $\beta$ Klotho knockdown in LNCaP cells. LNCaP cells were transfected with either control siRNA or  $\beta$ Klotho siRNA, followed by (A) a CCK-8 assay, (B) an apoptosis assay and (C) Transwell migration and invasion assays that were performed at the indicated times. (D) LNCaP cells were transfected with either control siRNA or  $\beta$ Klotho siRNA for 48 h, and western blotting was performed to detect the expression of  $\beta$ Klotho, E-cadherin, N-cadherin and vimentin. GAPDH was used as the loading control. (E) The morphology of LNCaP cells transfected with either control siRNA or  $\beta$ Klotho siRNA for 48 h. The cells were observed using phase contrast microscopy at x200 magnification. Scale bar, 50  $\mu$ m; \*P<0.05, \*\*P<0.01 vs. scrambled. Scrambled, control siRNA; siβKlotho,  $\beta$ Klotho siRNA.

further demonstrated by colony formation assays (Fig. 3B). A flow cytometric assay was performed to detect the effect of  $\beta$ Klotho on the apoptosis of PC3 cells. In cells transfected with  $\beta$ Klotho, the PE Annexin V<sup>+</sup>/7-AAD<sup>-</sup> (early apoptosis) subpopulation was significantly increased compared to the EV-transfected cells (Fig. 3C). The migration and invasion abilities of cells were determined using Transwell assays.  $\beta$ Klotho significantly inhibited the migration and invasion of PC3 cells (Fig. 3D). These results indicated that  $\beta$ Klotho overexpression inhibited the viability, migration and invasion, and promoted apoptosis of PC3 cells.

**$\beta$ Klotho overexpression reverses DHT-induced EMT through ERK1/2 signaling in PC3 cells.** To determine whether  $\beta$ Klotho is involved in the EMT regulation of PCa, we examined the expression of EMT-related markers in PC3-EV and PC3- $\beta$ Klotho cells with or without treatment of DHT using western blot analysis. As described above, concerning the effects of DHT on the EMT of PC3 cells, similar data were obtained in PC3-EV cells. DHT treatment significantly decreased the expression of E-cadherin, increased the expression of N-cadherin and vimentin in PC3-EV cells, and markedly induced the phosphorylation of ERK1/2 (Fig. 3E). However, the DHT-induced EMT phenotype was reversed in PC3- $\beta$ Klotho cells. Moreover,  $\beta$ Klotho alone increased the expression of E-cadherin and decreased the expression of N-cadherin and vimentin.  $\beta$ Klotho also inhibited DHT-induced phosphorylation of ERK1/2 in PC3 cells.

We next examined the effect of  $\beta$ Klotho on the morphology of PC3 cells. PC3 cells became concentrated, round and lost

their spindle-shaped morphology, which are characteristics of epithelial-like morphology, after transfection with  $\beta$ Klotho (Fig. 3F). Collectively, these data indicated that  $\beta$ Klotho overexpression reversed DHT-induced EMT through ERK1/2 signaling in PC3 cells.

**Knockdown of  $\beta$ Klotho promotes viability, migration, invasion and EMT, and inhibits apoptosis of LNCaP cells.** To further investigate the role of  $\beta$ Klotho in the EMT of PCa cells, we used siRNA to knock down the  $\beta$ Klotho in LNCaP cells, which have high endogenous expression of  $\beta$ Klotho. As expected, knockdown of  $\beta$ Klotho promoted the viability and inhibited the apoptosis of LNCaP cells (Fig. 4A and B). In addition, knockdown of  $\beta$ Klotho increased the migration and invasion abilities of the LNCaP cells (Fig. 4C). Moreover, western blot analysis revealed that the expression of E-cadherin was downregulated, and the expression of N-cadherin and vimentin was upregulated after  $\beta$ Klotho was knocked down in LNCaP cells (Fig. 4D). The cells became scattered, acquired spindle-shaped morphology and lost cell-cell contacts, which are characteristics of a mesenchymal-like morphology, after  $\beta$ Klotho was knocked down in LNCaP cells (Fig. 4E). Collectively, these results revealed that knockdown of  $\beta$ Klotho promoted viability, migration, invasion and EMT, and inhibited the apoptosis of LNCaP cells.

**$\beta$ Klotho overexpression inhibits tumor growth and EMT in vivo.** To further confirm the anti-viability and anti-EMT effects of  $\beta$ Klotho, we conducted a mice xenograft experiment. PC3-EV and PC3- $\beta$ Klotho cells were subcutaneously injected

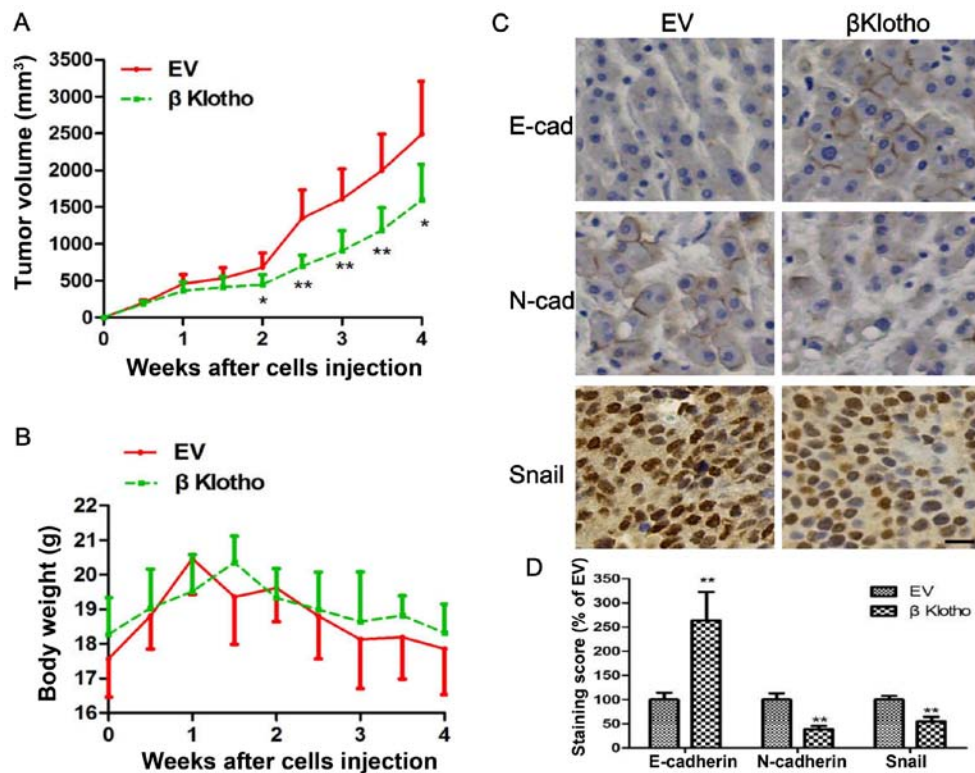


Figure 5.  $\beta$ Klotho overexpression inhibits tumor growth and EMT in PC3 cell xenografts. PC3 cells transfected with either EV or  $\beta$ Klotho were injected subcutaneously into the flanks of the BALB/c nude mice. (A) The tumor growth curve and (B) mice weight curve are depicted. (C) Immunohistochemical staining of E-cadherin, N-cadherin and Snail from the tumors of both groups. (D) Quantification of immunohistochemical score. Data are presented as the mean  $\pm$  SD. Each experiment was performed in duplicate or triplicate. Scale bar, 50  $\mu$ m. EMT, epithelial-mesenchymal transition. \*  $P < 0.05$ , \*\*  $P < 0.01$  vs. EV.

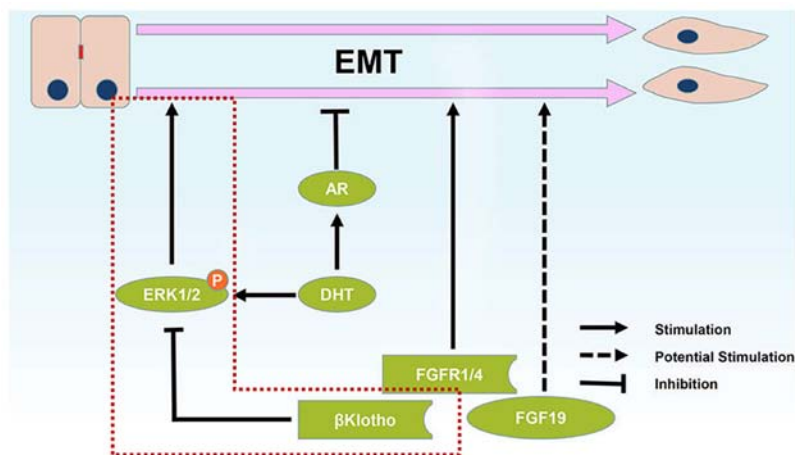


Figure 6. Schematic representation of the roles of FGF/FGFR/ $\beta$ Klotho signaling and AR signaling in epithelial-mesenchymal transition in prostate cancer. ERK phosphorylation was reported to induce the EMT process and our study revealed that  $\beta$ Klotho inhibited EMT of prostate cancer through inhibition of ERK phosphorylation. The  $\beta$ Klotho/ERK1/2/EMT axis is revealed in a red dotted line. AR, androgen receptor; EMT, epithelial-mesenchymal transition.

into the flank of each mouse, and the tumor growth and mouse body weight between the two groups was compared. We found that the volume of tumors induced by the PC3- $\beta$ Klotho cells was significantly smaller than that of PC3-EV cells (Fig. 5A). However, the mouse body weights between the two groups has no statistical difference (Fig. 5B). To reveal whether tumor cells *in vivo* have the signatures of the expression of genes similar to the *in vitro* experiments, we assessed the expression of selected genes related to EMT using immunohistochemistry. We found much more intense staining of E-cadherin

and less intense staining of N-cadherin and Snail in tumor tissues derived from PC3- $\beta$ Klotho compared with the PC3-EV cells (Fig. 5C and D). These data revealed that  $\beta$ Klotho inhibited the growth and EMT of xenograft tumors.

## Discussion

Continuous androgen receptor (AR) signaling activation remains the key attribute of CRPC (27). Epithelial-mesenchymal transition (EMT) is reported to have intimate



crosstalk with AR signaling and is known to be responsible for metastasis formation and CRPC. Our results indicated that androgen stimulation could induce the EMT phenotype in AR-negative PC3 cells, whereas in AR-positive LNCaP cells, this phenotype was not represented. The results are somewhat confusing, considering AR is a downstream factor of androgen stimulation. The possible explanation of this phenomena is that androgen exerts its function through both the AR-dependent and AR-independent pathways. For the AR-dependent pathways, androgen upregulates AR expression and promotes AR translocation to the nucleus to inactivate AR downstream gene transcription, such as Snail and Zeb1, resulting in the inhibition of EMT. These hypotheses are supported by the evidence that AR inhibits Snail and Zeb1 at both transcriptional and translational levels (4,12). For the AR-independent pathways, androgen can activate the pathways, such as ERK1/2 and PI3K/AKT, (28) leading to cell proliferation and EMT. This is supported by a study that revealed that ERK has direct interactions with vimentin and induces Slug phosphorylation in EMT initiation (29). In addition, Ichikawa *et al* (30) reported that ERK signaling contributes to the suppression of the E-cadherin gene during EMT. In the present study, we found that ERK1/2 was markedly phosphorylated after androgen stimulation in both PC3 and LNCaP cells. Moreover, after introduction of an ERK1/2 inhibitor, U0126, the androgen-induced EMT phenotype in PC3 cells was reversed, indicating that androgen induces EMT in prostate cancer (PCa) cells through the ERK1/2 pathway.

Collectively, the effects of androgen on the EMT phenotype may result from the combined effects of the AR-dependent and AR-independent pathways (Fig. 6). Therefore, all of these 3 results, EMT induction, EMT inhibition and EMT unaffectedness, are reasonable after androgen stimulation based on different contexts. Our results are generally in accordance with an earlier study that revealed that androgen treatment induced EMT in the context of AR absence (11), and a high AR content suppressed the androgen-induced EMT phenotype in PCa cells.

FGF/FGFR signaling is also involved in tumor progression and EMT in multiple tissue types. To further uncover the role of FGF/FGFR signaling in PCa, we examined its co-receptor,  $\beta$ Klotho, which is required for ligand binding and the activation of FGF/FGFR signaling. We found that  $\beta$ Klotho expression was significantly decreased in PCa tissues compared with that in BPH tissues. In addition, low  $\beta$ Klotho expression was associated with a high Gleason score of PCa. These results remind us that  $\beta$ Klotho may act as a tumor suppressor in tumorigenesis, which is in accordance with a recent study revealing that  $\beta$ Klotho expression was reduced in human non-melanoma skin cancer (31). Whether  $\beta$ Klotho can be a survival predictor of PCa needs to be further investigated in a study conducted with more patients.

Additional *in vitro* and *in vivo* studies using overexpression and knockdown techniques demonstrated that  $\beta$ Klotho inhibited viability, migration and invasion in PCa cells and inhibited tumor growth in a mouse model. In addition, we found that  $\beta$ Klotho induced apoptosis in PCa cells, which is consistent with the findings of Luo *et al* (32). They revealed that  $\beta$ Klotho interacts with FGFR4 to induce caspase-3-dependent

apoptosis and inhibit hepatoma cell proliferation. To the best of our knowledge for the first time, we revealed that  $\beta$ Klotho reversed androgen-induced and uninduced EMT in PCa cells and prostate tumors, which was likely reliant on the inhibition of ERK1/2 signaling, since ERK has been reported to contribute to EMT by affecting multiple EMT markers and EMT-related transcriptional factors (such as E-cadherin, vimentin, Slug and Snail) (29,30,33). Collectively, as an FGF/FGFR signaling co-receptor,  $\beta$ Klotho inhibited EMT and played a tumor-suppressive role in PCa. This may partly explain why FGF/FGFR signaling has tumor-suppressive functions in certain contexts.

In conclusion, our study demonstrated that  $\beta$ Klotho not only inhibited PCa cell growth but also inhibited the androgen/AR-associated EMT and the progression of prostate tumors through inactivation of the ERK1/2 signaling pathway (Fig. 6). The present study links FGF/FGFR/ $\beta$ Klotho signaling to the regulation of PCa progression, establishing  $\beta$ Klotho as a novel potential target for CRPC therapeutics.

## Acknowledgements

Not applicable.

## Funding

The present study was supported by grants from the National Natural Science Foundation of China (no. 81272858), the Shandong Province Key Research and Development Projects (nos. 2017GSF218070, 2016GSF201147 and 2016GSF201086), the Science and Technology Development Program of Jinan (no. 201506012) and the Shandong Province Medical and Health Technology Development Projects (nos. 2016WS0425 and 2016WS0442).

## Availability of data and materials

The data and materials are available from the corresponding author upon reasonable request.

## Author's contributions

HZ and JIL conceived and designed the study. ZL, SSQ, DQS, WD and LY performed the experiments. ZL and SL wrote the manuscript. MJL and XBZ reviewed and edited the manuscript. All authors read and approved the manuscript and agree to be accountable for all aspects of the research in ensuring that the accuracy or integrity of any part of the work are appropriately investigated and resolved.

## Ethics approval and consent to participate

All experimental protocols were approved by the Institutional Ethical Board of the Shandong Provincial Hospital Affiliated to Shandong University (Jinan, Shandong, China).

## Consent for publication

Not applicable.



## Competing interests

The authors declare that they have no competing interests.

## References

1. Siegel RL, Miller KD and Jemal A: Cancer statistics, 2017. *CA Cancer J Clin* 67: 7-30, 2017.
2. Scher HI, Halabi S, Tannock I, Morris M, Sternberg CN, Carducci MA, Eisenberger MA, Higano C, Bubley GJ, Dreicer R, *et al*: Design and end points of clinical trials for patients with progressive prostate cancer and castrate levels of testosterone: Recommendations of the prostate cancer clinical trials working group. *J Clin Oncol* 26: 1148-1159, 2008.
3. Li P, Yang R and Gao WQ: Contributions of epithelial-mesenchymal transition and cancer stem cells to the development of castration resistance of prostate cancer. *Mol Cancer* 13: 55, 2014.
4. Sun Y, Wang BE, Leong KG, Yue P, Li L, Jhunjhunwala S, Chen D, Seo K, Modrusan Z, Gao WQ, *et al*: Androgen deprivation causes epithelial-mesenchymal transition in the prostate: Implications for androgen-deprivation therapy. *Cancer Res* 72: 527-536, 2012.
5. Maeda M, Johnson KR and Wheelock MJ: Cadherin switching: Essential for behavioral but not morphological changes during an epithelium-to-mesenchyme transition. *J Cell Sci* 118: 873-887, 2005.
6. Zeisberg M and Neilson EG: Biomarkers for epithelial-mesenchymal transitions. *J Clin Invest* 119: 1429-1437, 2009.
7. Peinado H, Quintanilla M and Cano A: Transforming growth factor beta-1 induces snail transcription factor in epithelial cell lines: Mechanisms for epithelial mesenchymal transitions. *J Biol Chem* 278: 21113-21123, 2003.
8. Graham TR, Zhau HE, Otero-Marrah VA, Osunkoya AO, Kimbro KS, Tighiouart M, Liu T, Simons JW and O'Regan RM: Insulin-like growth factor-I-dependent up-regulation of ZEB1 drives epithelial-to-mesenchymal transition in human prostate cancer cells. *Cancer Res* 68: 2479-2488, 2008.
9. Kwok WK, Ling MT, Lee TW, Lau TC, Zhou C, Zhang X, Chua CW, Chan KW, Chan FL, Glackin C, *et al*: Up-regulation of TWIST in prostate cancer and its implication as a therapeutic target. *Cancer Res* 65: 5153-5162, 2005.
10. Qin Q, Xu Y, He T, Qin C and Xu J: Normal and disease-related biological functions of Twist1 and underlying molecular mechanisms. *Cell Res* 22: 90-106, 2012.
11. Zhu ML and Kyprianou N: Role of androgens and the androgen receptor in epithelial-mesenchymal transition and invasion of prostate cancer cells. *FASEB J* 24: 769-777, 2010.
12. Miao L, Yang L, Li R, Rodrigues DN, Crespo M, Hsieh JT, Tilley WD, de Bono J, Selth LA and Raj GV: Disrupting androgen receptor signaling induces snail-mediated epithelial-mesenchymal plasticity in prostate cancer. *Cancer Res* 77: 3101-3112, 2017.
13. Wu K, Gore C, Yang L, Fazli L, Gleave M, Pong RC, Xiao G, Zhang L, Yun EJ, Tseng SF, *et al*: Slug, a unique androgen-regulated transcription factor, coordinates androgen receptor to facilitate castration resistance in prostate cancer. *Mol Endocrinol* 26: 1496-1507, 2012.
14. Shiota M, Itsumi M, Takeuchi A, Imada K, Yokomizo A, Kuruma H, Inokuchi J, Tatsugami K, Uchiumi T, Oda Y and Naito S: Crosstalk between epithelial-mesenchymal transition and castration resistance mediated by Twist1/AR signaling in prostate cancer. *Endocr Relat Cancer* 22: 889-900, 2015.
15. Feng S, Dakhova O, Creighton CJ and Ittmann M: Endocrine fibroblast growth factor FGF19 promotes prostate cancer progression. *Cancer Res* 73: 2551-2562, 2013.
16. Acevedo VD, Gangula RD, Freeman KW, Li R, Zhang Y, Wang F, Ayala GE, Peterson LE, Ittmann M and Spencer DM: Inducible FGFR-1 activation leads to irreversible prostate adenocarcinoma and an epithelial-to-mesenchymal transition. *Cancer Cell* 12: 559-571, 2007.
17. Sugiyama N, Varjosalo M, Meller P, Lohi J, Hyytiäinen M, Kilpinen S, Kallioniemi O, Ingvarsen S, Engelholm LH, Taipale J, *et al*: Fibroblast growth factor receptor 4 regulates tumor invasion by coupling fibroblast growth factor signaling to extracellular matrix degradation. *Cancer Res* 70: 7851-7861, 2010.
18. Huang X, Yang C, Jin C, Luo Y, Wang F and McKeenhan WL: Resident hepatocyte fibroblast growth factor receptor 4 limits hepatocarcinogenesis. *Mol Carcinog* 48: 553-562, 2009.
19. Ricol D, Cappellen D, El Marjou A, Gil-Diez-de-Medina S, Girault JM, Yoshida T, Ferry G, Tucker G, Poupon MF, Chopin D, *et al*: Tumour suppressive properties of fibroblast growth factor receptor 2-IIIb in human bladder cancer. *Oncogene* 18: 7234-7243, 1999.
20. Yan G, Fukabori Y, McBride G, Nikolaropoulos S and McKeenhan WL: Exon switching and activation of stromal and embryonic fibroblast growth factor (FGF)-FGF receptor genes in prostate epithelial cells accompany stromal independence and malignancy. *Mol Cell Biol* 13: 4513-4522, 1993.
21. Kurosu H and Kuro OM: The Klotho gene family as a regulator of endocrine fibroblast growth factors. *Mol Cell Endocrinol* 299: 72-78, 2009.
22. Fu L, John LM, Adams SH, Yu XX, Tomlinson E, Renz M, Williams PM, Soriano R, Corpuz R, Moffat B, *et al*: Fibroblast growth factor 19 increases metabolic rate and reverses dietary and leptin-deficient diabetes. *Endocrinology* 145: 2594-2603, 2004.
23. Choi M, Moschetta A, Bookout AL, Peng L, Umetani M, Holmstrom SR, Suino-Powell K, Xu HE, Richardson JA, Gerard RD, *et al*: Identification of a hormonal basis for gallbladder filling. *Nat Med* 12: 1253-1255, 2006.
24. Ye X, Guo Y, Zhang Q, Chen W, Hua X, Liu W, Yang Y and Chen G:  $\beta$ Klotho suppresses tumor growth in hepatocellular carcinoma by regulating Akt/GSK-3 $\beta$ /cyclin D1 signaling pathway. *PLoS One* 8: e55615, 2013.
25. Liu Z, Qi S, Zhao X, Li M, Ding S, Lu J and Zhang G: Metformin inhibits 17 $\beta$ -estradiol-induced epithelial-to-mesenchymal transition via  $\beta$ Klotho-related ERK1/2 signaling and AMPK $\alpha$  signaling in endometrial adenocarcinoma cells. *Oncotarget* 7: 21315-21331, 2016.
26. Poh W, Wong W, Ong H, Aung MO, Lim SG, Chua BT and Ho HK: Klotho-beta overexpression as a novel target for suppressing proliferation and fibroblast growth factor receptor-4 signaling in hepatocellular carcinoma. *Mol Cancer* 11: 14, 2012.
27. Robinson D, Van Allen EM, Wu YM, Schultz N, Lonigro RJ, Mosquera JM, Montgomery B, Taplin ME, Pritchard CC, Attard G, *et al*: Integrative clinical genomics of advanced prostate cancer. *Cell* 161: 1215-1228, 2015.
28. Liao RS, Ma S, Miao L, Li R, Yin Y and Raj GV: Androgen receptor-mediated non-genomic regulation of prostate cancer cell proliferation. *Transl Androl Urol* 2: 187-196, 2013.
29. Virtakoivu R, Mai A, Mattila E, De Franceschi N, Imanishi SY, Corthals G, Kaukonen R, Saari M, Cheng F, Torvaldsen E, *et al*: Vimentin-ERK signaling uncouples Slug gene regulatory function. *Cancer Res* 75: 2349-2362, 2015.
30. Ichikawa K, Kubota Y, Nakamura T, Weng JS, Tomida T, Saito H and Takekawa M: MCRIP1, an ERK substrate, mediates ERK-induced gene silencing during epithelial-mesenchymal transition by regulating the co-repressor CtBP. *Mol Cell* 58: 35-46, 2015.
31. Nakai K, Yoneda K, Haba R, Kushida Y, Katsuki N, Moriue J, Moriue T, Koura A, Yokoi I, Ishikawa E, *et al*: [beta]Klotho expression is reduced in human non-melanoma skin cancer. *Int J Dermatol* 54: e431-e433, 2015.
32. Luo Y, Yang C, Lu W, Xie R, Jin C, Huang P, Wang F and McKeenhan WL: Metabolic regulator betaKlotho interacts with fibroblast growth factor receptor 4 (FGFR4) to induce apoptosis and inhibit tumor cell proliferation. *J Biol Chem* 285: 30069-30078, 2010.
33. Zhao J, Ou B, Han D, Wang P, Zong Y, Zhu C, Liu D, Zheng M, Sun J, Feng H and Lu A: Tumor-derived CXCL5 promotes human colorectal cancer metastasis through activation of the ERK/Elk-1/Snail and AKT/GSK3 $\beta$ / $\beta$ -catenin pathways. *Mol Cancer* 16: 70, 2017.



This work is licensed under a Creative Commons Attribution-NonCommercial-NoDerivatives 4.0 International (CC BY-NC-ND 4.0) License.